External and internal constraints on eukaryotic chemotaxis

Danny Fuller<sup>1\*</sup>, Wen Chen<sup>2\*</sup>, Micha Adler<sup>2</sup>, Alex Groisman<sup>2</sup>, Herbert Levine<sup>2,3</sup>, Wouter-Jan Rappel<sup>2,3</sup>, William F. Loomis<sup>1</sup>

- 1 Cell and Developmental Biology, Division of Biological Sciences,
- 2 Department of Physics and
- 3 Center for Theoretical Biological Physics, University of California San Diego, La Jolla, CA 92093
- \*These authors contributed equally to this work

#### Abstract

Chemotaxis, the chemically guided movement of cells, plays an important role in a number of biological processes including cancer, wound healing and embryogenesis. Chemotacting cells are able to sense shallow chemical gradients where the concentration of chemoattractant differs by only a few percent from one side of the cell to the other, over a wide range of local concentrations. Exactly what limits the chemotactic ability of these cells is presently unclear. Here we determine the chemotactic response of *Dictyostelium* cells to exponential gradients of varying steepness and local concentration of the chemoattractant cAMP. We find that the cells are sensitive to the steepness of the gradient as well as to the local concentration. Using information theory techniques, we derive a formula for the mutual information between the input gradient and the spatial distribution of bound receptors and also compute the mutual information between the input gradient and the motility direction in the experiments. A comparison between these two quantities reveals that for shallow gradients, in which the concentration difference between the back and the front of a 10 µm diameter cell is less than 5 %, and for small local concentrations (less than 10 nM) the intracellular information loss is insignificant. Thus, external fluctuations due to the finite number of receptors dominate and limit the chemotactic response. For steeper gradients and higher local concentrations, the intracellular information processing is sub-optimal and results in a much smaller mutual information between the input gradient and the motility direction than would have been predicted from the ligand-receptor binding process.

\body

## Introduction

Chemotaxis, the motion of cells guided by chemical gradients, plays an important role in a variety of biological processes, including wound healing, embryogenesis and cancer metastasis. The chemical gradients required for efficient chemotaxis can be very shallow for eukaryotic cells. For example, the rapidly crawling neutrophils of the mammalian immune system and the social amoebae, *Dictyostelium discoideum* (1-8), are able to sense shallow chemical gradients where the concentration of chemoattractant differs by only a few percent from one side of the cell to the other, over a wide range of local concentrations (9-11).

The chemotactic response of these cells can be considered as the outcome from two distinct steps: establishment of spatial differences in the distribution of receptors with bound chemoattractant on the cell's surface (12) and the response to these differences by the signal transduction pathways leading to directed motility (13). The first step is subject to the external fluctuations in chemoattractant binding to the surface receptor. This external noise can be precisely characterized, either through direct numerical simulations (14, 15) or through approximate analytical calculations (16-18). The second step involves a number of pathways that are subject to internal background noise generated by any of the components that drive the extension and retraction of pseudopods leading to cell movement. Furthermore, these pathways can operate in a nonlinear fashion that can reduce the amount of intracellular information transfer. The internal noise and the effect of the nonlinearity of the pathways are difficult to quantify. Multiple signaling pathways

operating in parallel, each with a number of unknown components, determine the direction of movement. The quantification of noise necessitates knowledge about the number of involved molecules, their reaction rates and their diffusion constants while quantifying the signal processing of the nonlinear pathways requires a detailed and complete mechanistic motility model.

In this study, we investigate the chemotactic response of *Dictyostelium* cells in stable exponential chemoattractant gradients generated in microfluidics devices. Using this experimental data, we compute the mutual information between the external gradient direction and the motility direction, which is a measure of the information that these variables share (19). We also calculate analytically the mutual information between the external gradient and the spatial distribution of bound receptors. A comparison of these two quantities allows us to evaluate when the chemotactic response is being limited by sensing noise, (assuming that the directional motility response is indicative of the goal of the chemotactic process), or alternatively by suboptimal intracellular processing of the information from the bound receptors.

#### Results

## Quantitative experimental studies of chemotaxis

We performed quantitative experiments of developed *Dictyostelium* cells in exponential cAMP gradients using microfluidic devices. Within these devices, we can define a difference of the concentration between the front and the back of the cells,  $\Delta C$ , along with the local concentration experienced by the cell,  $C_{local}$ . The choice of an exponential gradient ensures that the proportional concentration difference, i.e. the ratio  $\Delta C/C_{local}$ , is independent of the position in the device. Furthermore, the fluid flow within the microfluidic devices guarantees that signaling between cells can be neglected. An example of an exponential gradient in the microfluidic devices using a fluorescent dye is shown in Fig. 1a.

We examined the chemotactic response as a function of the two gradient parameters:  $C_{local}$ , and the gradient steepness, p, which can be expressed as the percent difference in concentration between the front and the back. We used devices that generated gradients of different steepnesses, ranging from a 1.25% to a 10% difference in concentration across a cell with a diameter of L=10  $\mu$ m, and tracked the paths of cells over a period of 8 minutes. The chemotactic index (CI) was calculated as the ratio of the distance covered in the direction of the gradient and the total distance traveled. Cell tracks in a representative steep and shallow gradient are shown in Fig. 1b-c. In the steep gradient (10%, Fig. 1b), most cells move in the direction of the gradient and the CI for this experiment was 0.56. On the other hand, in the shallow gradient (1.25%, Fig. 1c) there was no detectable directional bias, resulting in a CI that is indistinguishable from 0.

The chemotactic response was determined in devices that generated gradients with 5 different steepnesses (Fig. 2a). Cells that were exposed to an average local concentration in a 1-10nM range are shown as circles while cells with an average local concentration within 10-30nM are plotted as squares. For the 1-10nM concentration range, the cells failed to recognize the shallowest gradient (1.25%) but responded with increasingly accurate directionality to the steeper gradients (2.5% to 10%) with a maximum CI that is consistent with previous reports (20).

To investigate the effect of the local concentration on the CI we systematically varied the concentration range in a 1.25% and a 2.5% exponential gradient and report the CI as a function of the geometric mean of the minimal and maximal local concentration within the microfluidic device  $\overline{C}_{local}$  (Fig. 2b). For a 1.25% gradient, the CI increases for increasing average local concentration, reaches a maximum around  $\overline{C}_{local} \sim 15$ nM and decreases upon further increasing the local concentration. The dependence of the CI on the local concentration in a 2.5% gradient is qualitatively similar but peaks at a smaller local concentration. Thus, our experiments indicate that the maximum CI is reached well below the reported value for the receptor dissociation constant  $K_d=30$ nM (21).

### Analysis using information theoretic techniques

To quantify the fluctuations originating from the external binding process we first computed the mutual information (22) between the external chemoattractant gradient direction  $\theta_s$  and the resulting spatial distributions of bound receptors *Y*. This mutual information is a measure of how much the uncertainty in *Y* is reduced by the knowledge of  $\theta_s$ . It is typically expressed in units of bits and is always equal or larger than 0: a mutual information equal to 0 implies that knowing the external gradient direction does not reduce the uncertainty in the spatial distribution of bound receptors.

We considered a circular two-dimensional cell, divided the cell membrane into n segments containing an equal number of N/n receptors, where N is the total number of receptors, and considered simple first-order ligand-receptor kinetics. An exact formula

for this external mutual information  $I(Y; \theta_s)$  for a single measurement is derived in the Supporting Information and for shallow gradients this reduces to

$$I(Y;\theta_s) \approx \frac{NK_d C_{local} p^2}{16\ln(2) (K_d + C_{local})^2}$$
[1]

where  $K_d$  is the dissociation constant of the ligand-receptor binding process. Thus, the external mutual information has a maximum at a local concentration equal to  $K_d$  and the value of this maximum only depends on the number of receptors and on the gradient steepness. Our choice of equal numbers of receptors per segment was motivated by experimental data which show a homogeneous spatial distribution of receptors on the membrane (23, 24). The case of randomly placed receptors, leading to a variable number of receptors in each segment, is analyzed in the Supporting Information. We found that the mutual information in this case is almost identical to the mutual information found using Eq. [1]. In the Supporting Information we also discuss the mutual information for elliptical cells and show that the mutual information can increase only by a modest amount (~20%) for highly elongated cells.

To determine how much additional information is lost in the internal processing steps, we computed the mutual information  $I(\theta_r; \theta_s)$  between the gradient direction  $\theta_s$  and the motility direction  $\theta_r$ . This mutual information determines how much information an observer of the cell motion has about the gradient direction, and takes into account both the external and the internal steps. It follows from the data processing inequality that it can be at most equal to the external mutual information. We determined, for each experiment, the instantaneous response angle  $\theta_r$  for all cell tracks. Next, we divided the  $360^0$  range of  $\theta_r$  in *m* bins and computed the fraction of angles falling within each bin,  $N_j$ . The choice of the number of bins was optimized using a procedure which minimizes a cost function that is a measure of the error introduced by binning the data (25) (see Supporting Information). The resulting histogram of  $\theta_r$  using the optimal bin size is shown in Fig. 3a for a 10% gradient. Then, the external and internal mutual information was calculated as

$$I(\theta_r; \theta_s) = \sum_{j=1}^m N_j \log N_j + \log m \quad [2]$$

(see Supporting Information for more details). In Fig. 3b we show this mutual information as a function of the gradient steepness, along with the numerically determined external mutual information and in Fig. 3c we show these quantities as a function of  $\overline{C}_{local}$  for a gradient of 2.5%. The error bars in the external and internal mutual information are due to the finite number of data points and the range of local concentrations to which the cells are exposed.

#### Discussion

Recently, the role of fluctuations in chemotaxis has received significant attention (15, 16, 18, 20, 26, 27). Most studies, however, were either purely theoretical or were performed under conditions that were difficult to quantify. Our approach, which uses exponential gradients generated in microfluidic devices, has several benefits. It allows us to precisely quantify the gradient presented to the cells, since the exponential profile ensures that the fractional concentration difference is independent of the position in the device. Moreover, the fluid flow abolishes any potential cell-to-cell signaling. The main parameters that determine the gradient (the steepness and the local concentration) can be controlled in each device, allowing us to fix one and vary the other.

Our experiments in which the local concentration was restricted to a narrow range show that the CI increases for increasing gradient steepness (Fig 2A). These results are in agreement with recent theoretical investigations of the directional sensing process that predict a sigmoidal dependence of the CI on the gradient steepness (16, 27). Our results also indicate that the minimum gradient steepness required for a directional response depends on the local concentration: cells exposed to a 1.25% do not respond directionally in a 1-10nM concentration range but do respond in a 10-30nM concentration range. Hence, chemotaxis is controlled by both the gradient steepness and the local concentration. This is further illustrated when we keep the gradient steepness constant and vary the local concentration (Fig. 2B). The dependence of the CI on the local concentration in both a 1.25% and a 2.5% gradient is qualitatively similar. However, the CI in the 2.5% gradient peaks at a smaller local concentration. Thus, our experiments indicate that the maximum CI is reached well below the reported value for the receptor dissociation constant  $K_d$ =30nM (21).

To characterize the fluctuations originating from the external binding process we computed the mutual information between the external chemoattractant gradient direction  $\theta_s$  and the resulting spatial distributions of bound receptors *Y*. The result shows that this external mutual information has a maximum when the local concentration equals  $K_d$ . A similar result was also found from a signal-to-noise analysis (15). In other words, based purely on the spatial distribution of bound receptors, chemotaxing cells would perform ideally when the local concentration is equal to the dissociation constant. The optimal local concentration for neutrophils in an exponential gradient was also determined to be around  $K_d$  (10) while an analysis in which receptors are randomly distributed can reduce

the optimal concentration by at most 50% (26). Thus, our experiments, combined with this theoretical analysis, suggest that the processing of the gradient cues inside cells reduce the optimal local concentration for chemotaxis and that this optimal concentration is determined through a convolution of the external (i.e., receptor binding and unbinding) and internal steps (27).

This conclusion is unchanged when one takes into account that Eq. [1] is valid for a single "snapshot" measurement and needs to be modified to include multiple independent measurements of the receptor binding distribution. A typical correlation time for this distribution can be calculated (15) using experimentally measured off rates (12) and is around 5s, which is comparable to the pseudopod life time. In the Supporting Information, we show that this leads to an estimated prefactor of order 1.

For shallow gradients (< 5%) we find that the external mutual information is comparable to the mutual information for the entire chemotactic process (Fig. 3b). This means that the information lost in intracellular signal pathways is negligible and that the intracellular information processing is near optimal. In other words, the receptor-ligand binding noise dominates the chemotactic process and determines the precision of the cells in shallow gradients. Implicit in reaching this conclusion is the assumption that the chemotactic process is evolutionarily designed to allow the cells to track the gradient direction as accurately as possible. For steeper gradients, on the other hand, the amount of information lost due to internal fluctuations is significant and can be as high as 1.5 bits. A comparison between the two mutual informations for a fixed gradient (Fig 3c) reveals that they are comparable for small local concentrations. For large (>10nM) concentrations, however, the external mutual information is much larger than the external and internal mutual information. Thus, we conclude that for steep gradients and for high local concentrations the intracellular information processing is sub-optimal and that intracellular pathways leading from the receptor to the establishment of a leading edge determine the chemotactic limits. For shallow gradients and low local concentrations, on the other hand, the receptor-ligand fluctuations limit the chemotactic efficiency.

A possible interpretation of our results comes from realizing that the optimal local concentration for the receptor-ligand process is at  $K_d$ . This suggests that the intracellular signaling networks have an optimal concentration well below this value. Increasing the steepness of the gradient increases the difference in the number of bound receptors between the front and the back of the cell. This could enlarge the relative contribution of the internal pathways, shifting the optimal local concentration to smaller values. The mechanisms behind the observed intracellular information loss are unclear. One possibility is that intracellular fluctuations become larger and limit the information transfer. Another possibility is that the signaling pathways are nonlinear and saturate for steep gradients and large concentrations, leading to a reduction in transfer of information. The latter possibility can be studied using existing models for directional sensing (15) and is currently under investigation.

#### **Materials and methods**

#### Growth and Development

Transformed AX4 cells carrying integrated constructs in which the regulatory region of actin 15 drives genes encoding a fusion of GFP to LimE as well as a gene

encoding a fusion of RFP to coronin (*LimE-GFP/corA-RFP*) were a gift from Richard Firtel and were used in all the experiments. The cells were grown in suspension in HL5 medium (28). Only cultures with mass doubling times less than 10 hrs were used since we found that slower growing cells were less chemotactically responsive. When exponentially growing cells reached 1-2 x 10<sup>6</sup> cells/ml, they were harvested by centrifugation, washed in KN2/Ca buffer (14.6 mM KH<sub>2</sub>PO<sub>4</sub>, 5.4 mM Na<sub>2</sub>HPO<sub>4</sub>, 100  $\mu$ M CaCl<sub>2</sub>, pH 6.4), and resuspended in KN2/Ca at 10<sup>7</sup> cells/ml. Shaken cells were developed for 5hrs with pulses of 50nM cAMP added every 6 minutes.

#### <u>Chemotaxis</u>

Developed cells were harvested, diluted 1:3 in KN2/Ca, and loaded into the microfluidics test chamber via syringe/blunt canula. Prior to the introduction of the preformed cAMP gradient the cells were in a continous flow of fresh KN2/Ca buffer to prevent establishment of self-generated cAMP gradients. They were allowed to settle and disperse on the coverslip for 15-30 minutes before imaging. Most cells at this time had a length to width ratio >3 and appeared to be polarized. Differential Interferance Contrast (DIC) images were taken on a Zeiss Axio Observer inverted microscope using a 10X objective and a Roper Cascade QuantEM 512SC camera. Frames were captured and analyzed using Slidebook 4 (Intelligent Imaging Innovations, Inc.).

Alexa594 (Invitrogen) fluorescent dye was added to the cAMP solutions used to form the gradients in direct proportion to the concentration of cAMP. Fluorescent images were taken periodically to record the actual shape and stability of the exponential gradients in the various microfluidic devices. Only devices which generated gradients with good correlation to exponential gradients across the field of capture were used. DIC images were captured every 5 seconds for 1500 seconds. The cAMP gradients were introduced at frame 20 and maintained through 300 captures. Analysis of chemotaxis was performed on frames 150 through 250.

## Quantitative measurement of cell movement

The centroids of all cells in the field were automatically tracked for 100 frames. Cells which moved the furthest without encountering another cell were chosen for data analysis. Ten to twenty-five such cells were found in each experiment. The average local concentration was determined for each cell by the average of the local concentration at the beginning and end of the track. The chemotactic index (CI) was calculated by dividing the distance traveled up gradient by the total distance traveled. On average, cells moved at the rate of  $15 \pm 2$  µm/minute irrespective of the steepness of the gradient or the local concentration. Each experiment was carried out 3 or 4 times on separate days and the chemotactic indices of the cells were averaged. The error bars in the figures represent the standard error of the mean. The instantaneous angle was determined from the positions of the centroid in successive frames.

Microfluidic devices used in the study were similar to those in recent experiments on the chemotaxis of neutrophil-like HL60 cells (10). Each device has three inlets for cAMP solutions with three different concentrations, one main outlet, two auxiliary ports, and a network of 30 µm deep microchannels with rectangular cross-sections. The device contains a gradient-maker, which generates an exponential concentration profile, and a 800 µm wide channel in which cells can be observed. The channel flow velocity is ~200 µm/s, and a 550 µm wide stream carrying an exponential gradient is flanked by two 125 µm streams with uniform concentrations, which are the minimal and maximal

concentrations in the gradient. In the 5 devices used in the study, the concentration varied by factors of 2, 4, 16, 64, and 256 across the 550  $\mu$ m wide gradient, corresponding to a 1.25, 2.5, 5, 7.5, and 10% variations across 10  $\mu$ m. One of the auxiliary ports of the device helps to fill the microchannels while the other auxiliary port enables the rapid establishment of a well-defined exponential.

## Acknowledgements

This work was supported by the US National Institutes of Health (PO1 GM078586). We wish to thank Johan Paulsson, Ph.D., for useful comments.

# References

- 1. Weiner OD, *et al.* (1999) Spatial control of actin polymerization during neutrophil chemotaxis. *Nat Cell Biol* 1(2):75-81.
- 2. Parent CA & Devreotes PN (1999) A cell's sense of direction. *Science* 284:765-770.
- 3. Geiger J, Wessels D, & Soll DR (2003) Human polymorphonuclear leukocytes respond to waves of chemoattractant, like Dictyostelium. *Cell Motil. Cytoskel*. 56:27-44.
- 4. Soll DR, Wessels D, Heid PJ, & Zhang H (2002) A contextual framework for characterizing motility and chemotaxis mutants in Dictyostelium discoideum. *J. Muscle Res. Cell Motil.* 23:659-672.
- 5. van Haastert PJM & Devreotes PN (2004) Chemotaxis: signalling the way forward. *Nature Rev. Mol. Cell Biol.* 5:626-634.
- 6. Charest PG & Firtel RA (2007) Big roles for small GTPases in the control of directed cell movement. *Biochem J* 401(2):377-390.
- 7. Weiner OD, *et al.* (2006) Hem-1 complexes are essential for Rac activation, actin polymerization, and myosin regulation during neutrophil chemotaxis. (Translated from eng) *PLoS Biol* 4(2):e38 (in eng).
- 8. Bosgraaf L & Van Haastert PJ (2009) The ordered extension of pseudopodia by amoeboid cells in the absence of external cues. (Translated from eng) *PLoS ONE* 4(4):e5253 (in eng).
- 9. Song L, *et al.* (2006) Dictyostelium discoideum chemotaxis: Threshold for directed motion. *Eur J Cell Biol* 85:981-989.
- 10. Herzmark P, *et al.* (2007) Bound attractant at the leading vs. the trailing edge determines chemotactic prowess. (Translated from eng) *Proc Natl Acad Sci U S A* 104(33):13349-13354 (in eng).
- 11. Devreotes PN & Zigmond SH (1988) Chemotaxis in eukaryotic cells: A focus on leukocytes and Dictyostelium. *Annu. Rev. Cell Biol.* 4:649-686.
- 12. Ueda M, Sako Y, Tanaka T, Devreotes P, & Yanagida T (2001) Single-molecule analysis of chemotactic signaling in Dictyostelium cells. *Science* 294:864-867.
- 13. Franca-Koh J, Kamimura Y, & Devreotes P (2006) Navigating signaling networks: chemotaxis in Dictyostelium discoideum. *Curr Opin Genet Dev* 16(4):333-338.
- 14. Wang K, Rappel WJ, Kerr R, & Levine H (2007) Quantifying noise levels of intercellular signals. *Phys Rev E Stat Nonlin Soft Matter Phys* 75(6 Pt 1):061905.
- 15. Rappel WJ & Levine H (2008) Receptor noise limitations on chemotactic sensing. *Proc Natl Acad Sci U S A* 105(49):19270-19275.
- 16. Endres RG & Wingreen NS (2008) Accuracy of direct gradient sensing by single cells. (Translated from eng) *Proc Natl Acad Sci U S A* 105(41):15749-15754 (in eng).
- 17. Berg HC & Purcell EM (1977) Physics of chemoreception. *Biophys J* 20:193-219.

- Bialek W & Setayeshgar S (2005) Physical limits to biochemical signaling. (Translated from eng) *Proc Natl Acad Sci U S A* 102(29):10040-10045 (in eng).
- 19. Cover TM & Thomas JA (2005) *Elements of Information Theory* (Wiley) 2nd Ed.
- 20. van Haastert PJ & Postma M (2007) Biased random walk by stochastic fluctuations of chemoattractant-receptor interactions at the lower limit of detection. *Biophys J* 93(5):1787-1796.
- 21. van Haastert PJM (1983) Binding of cAMP and adenosine derivatives to Dictyostelium discoideum cells. *J. Biol. Chem.* 258:9643-9648.
- Andrews BW & Iglesias PA (2007) An information-theoretic characterization of the optimal gradient sensing response of cells. *PLoS Comput. Biol.* 3(8):e153:1489-1497.
- 23. Xiao Z, Zhang N, Murphy DB, & Devreotes PN (1997) Dynamic distribution of chemoattractant receptors in living cells during chemotaxis and persistent stimulation. *J. Cell Biol.* 139:365-374.
- 24. Jin T, Zhang N, Long Y, Parent CA, & Devreotes PN (2000) Localization of the G protein betagamma complex in living cells during chemotaxis. *Science* 287:1034-1036.
- 25. Shimazaki H & Shinomoto S (2007) A method for selecting the bin size of a time histogram. (Translated from eng) *Neural Comput* 19(6):1503-1527 (in eng).
- 26. Mortimer D, *et al.* (2009) Bayesian model predicts the response of axons to molecular gradients. (Translated from eng) *Proc Natl Acad Sci U S A* 106(25):10296-10301 (in eng).
- 27. Rappel WJ & Levine H (2008) Receptor noise and directional sensing in eukaryotic chemotaxis. (Translated from eng) *Phys Rev Lett* 100(22):228101 (in eng).
- 28. Sussman M (1987) Cultivation and synchronous morphogenesis of Dictyostelium under controlled experimental conditions. *Meth. Cell Biol.* 28:9-29.

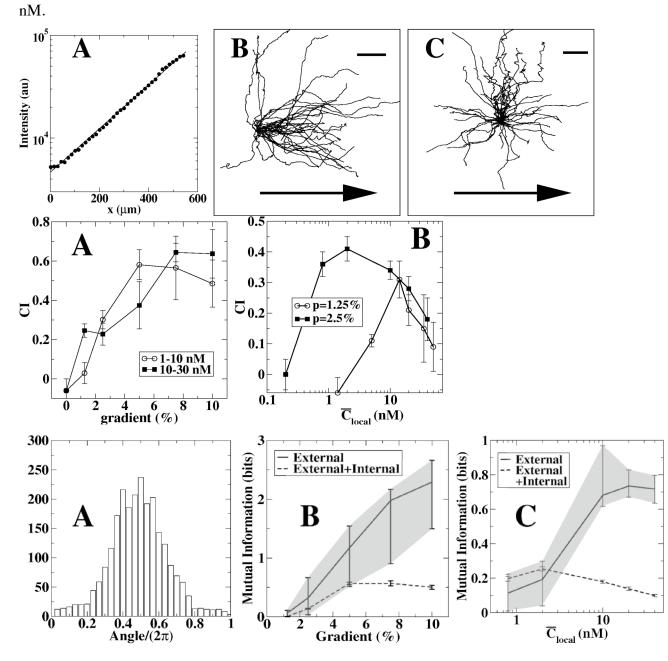
Figure Legends

**Figure 1.** The chemotactic response of cells in exponential gradients depends on the gradient steepness. **a**, The concentration as a function of the position along the gradient direction in the microfluidic device. The exponential gradient spans a 550 µm wide

region and the concentration can be described by  $C_{local}(x) = C(0)e^{\frac{p}{L}x}$  where  $L=10 \,\mu\text{m}$  and p is a measure of the steepness of the gradient. The steepness is expressed as the fractional difference in the concentration over 10  $\mu\text{m}$  and measures 5% for the data shown. **b-c**, Typical cell tracks, with their origins brought to a common point, are shown for a steep (10 %) gradient where the concentration within the microfluidic device varies between 1 nM and 256 nM (**b**) and for a shallow gradient (1.25 %) where the concentration spans values between 1 nM and 2 nM (**c**). The arrow indicates the direction of the gradient and the scale bars represent 20  $\mu\text{m}$ .

**Figure 2.** Dependence of the chemotactic index, CI, on the gradient steepness and the local concentration. **a**, Mean value of the CI as a function of the gradient steepness for cell migration trajectories with an average local concentration between 1nM and 10nM (circles) and between 10nM and 30nM (squares). **b**, The CI as a function of the local concentration for two different values of the gradient steepness. Each data point is an average value for cells exposed to local concentrations in a 2-fold (for p = 1.25%) or 4-fold (for p = 2.5%) range, with the plotted value of  $\overline{C}_{local}$  corresponding to the geometric mean of the range. In both figures, the error bars represent the standard error of the mean.

**Figure 3.** Dependence of the mutual information MI on the gradient parameters. **a**, Histogram of the instantaneous response angle  $\theta_r$  for the cell tracks in a 10% gradient, showing a pronounced peak at  $\theta_r = \pi$ , the gradient direction. **b-c**, The external and internal MI between the input gradient angle,  $\theta_s$ , and  $\theta_r$  calculated using the experimental data (dashed lines), and the external MI between  $\theta_s$  and the spatial distribution of bound receptors *Y*, calculated numerically (solid lines), as a function of the gradient steepness for cells with an average local concentration between 1nM and 10nM (**b**) and as a function of the mean local concentration for a 2.5% gradient (**c**). Parameters used for the



computation of the external MI are N=70,000 and  $K_d=30$